Fluorescence-Quenching Study of Percolation and Compartmentalization in Two-Phase Lipid Bilayers

Barbora Piknová,* Derek Marsh,# and Thomas E. Thompson*
*Department of Biochemistry, University of Virginia, Charlottesville, Virginia 22908 USA and #Max Planck Institut für Biophysikalische Chemie, D-37077 Göttingen, Germany

ABSTRACT Fluorescence quenching of a lipid-labeled fluorophore by a lipid spin-labeled quencher has been studied experimentally in two-component, two-phase phosphatidylcholine bilayers to examine the effect of phase connection and disconnection on quenching. Both fluorophore and quencher prefer the fluid phase. At the percolation threshold, the point at which the fluid phase becomes subdivided into many small disconnected domains, the quenching drops abruptly. This decrease in quenching is a function of the fluid-phase fraction and is due to the heterogeneous distribution of fluorophores and quenchers over the fluid-phase domains. Computer simulations of the system were carried out with a triangular lattice divided into closed compartments of variable size and reactant occupancy. The simulations demonstrate that the degree of quenching is reduced in the disconnected systems and that the reduction is correlated with the size of the disconnected domains. The combination of experimental data with simulations leads to the conclusion that at constant temperature the size of fluid-phase domains, n_{fluid}, in the region of the coexistence of the fluid and gel phases is proportional to the fluid fraction, X_{fluid}. This is in a qualitative agreement with a previous electron spin resonance study of interlipid spin–spin interactions in the same two-component, two-phase bilayer system.

INTRODUCTION

During the past 10 years knowledge about the organization of biological membranes has increased considerably. The early model of Singer and Nicolson (1972) considered the membrane as a continuous fluid mosaic of lipids and proteins. It was subsequently shown that the plasma membrane is organized in a domain structure (Pagano and Sleight, 1985; Tocanne et al., 1989; de Bony et al., 1989; Edidin and Stroynowski, 1991; Edidin, 1992). Although the physical basis for this structure is not clearly understood, recent evidence suggests the phase structure of the lipid bilayer component makes a contribution (for references see Tocanne, 1992; Welti and Glaser, 1994).

We have taken the view that the percolation properties of this domain structure, if under the control of the cell, can be used to govern the extent and the rate of molecular reactions and interactions in the plane of the cell membrane. This will be the case, provided that the average surface concentrations of the interactant molecules are small, as is the case for almost all biochemically active membrane molecules (Thompson et al., 1992; Melo et al., 1992; Thompson et al, 1995). This idea has been examined experimentally in a study of the spin–spin interaction between the spin-labeled phospholipids in a two-phase, two-component bilayer (Sankaram et al., 1992).

Here we present a further experimental examination of this idea, using a simple fluorophore–quencher interaction confined in a two-phase, two-component phospholipid bilayer composed of dimyristoylphosphatidylcholine (DMPC) and distearoylphosphatidylcholine (DSPC). The phase diagram for the system is well known, and the percolation threshold locus has been determined by fluorescence recovery after photobleaching and EPR (Vaz et al., 1989, Sankaram et al., 1992, Vaz, 1994). In this study the fluorophore, diphenylhexatriene phosphatidylcholine (DPH-PC), and the quencher, spin-labeled DMPC (SL-DMPC), are examined. The distributions between the fluid and gel phases of both quencher and fluorophore are known. The fluid–gel distribution constant, $K_{f/g} = 3.3$, for DPH-PC was measured by Parente and Lentz (1985) in different DMPC–DSPC mixtures and at different temperatures. SL-DMPC partitions between both phases in the same way as unlabeled DMPC (Sankaram et al., 1992), and so its distribution is simply given by the DMPC–DSPC phase diagram.

The results of the study show that at the percolation threshold, the point at which the fluid phase becomes discontinuous, quenching drops abruptly. This result is examined by computer simulations based on an earlier idea (Melo et al., 1992).

MATERIALS AND METHODS

Materials

DMPC, DSPC, and DPH-PC were purchased from Avanti Polar Lipids (Alabaster, AL) and were used without further purification. DMPC was synthesized as previously described (Marsh and Watts, 1982). The con-

Received for publication 8 March 1966 and in final form 3 May 1996

Address reprint requests to Dr. Thomas E. Thompson, Department of Chemistry, School of Medicine, University of Virginia, Box 440, Charlotesville, VA 22908. Tel.: 804-924-2651; Fax: 804-924-5069; E-mail: tet@virginia.edu.

Abbreviations used: DMPC, dimyristoylphosphatidylcholine; DSPC, distearoylphosphatidylcholine; DPPC, dipalmitoylphosphatidylcholine; DPH-PC,(1-palmitoyl-[[2-[4-(6-phenyl-*trans*-1, 3, 5-hexatrienyl)phenyl]-ethyl]-carbonyl]-3-*sn*-phosphatidylcholine; SL-DMPC or ^{13}SL-DMPC, 1-myristoyl-2-[13-(4, 4-dimethyloxazolidine-*N*-oxyl)]-myristoyl-*sn*-glycero-3-phosphocholine; ^{6}SL-DMPC, 1-myristoyl-2-[6-(4, 4-dimethyloxazolidine-*N*-oxyl)]-myristoyl-*sn*-glycero-3-phosphocholine; FRAP, fluorescence recovery after photobleaching.

0006-3495/96/08/892/06 $2.00

centration of spin label in the stock solution of SL-DMPC was determined by electron paramagnetic resonance.

Liposome preparation

Large unilamellar liposomes made from a mixture of DMPC and DSPC at various DMPC/DSPC molar ratios (0, 0.3, 0.4, 0.5, 0.6, 0.7, and 1.0) were prepared by extrusion of lipid multilayers as follows: The required amounts of DMPC and DSPC (usually ~0.2 mg/sample), fluorophore, and quencher were dissolved together in 500 μl of chloroform. In all samples the molar ratio of DPH-PC/total PC was 0.002. Systems were studied with molar ratios of SL-DMPC/total PC equal to 0, 0.00008, 0.0002, 0.0004, 0.0008, 0.002, 0.004, 0.008, 0.02, 0.04, 0.08. Chloroform was removed on a rotary vacuum evaporator to created a thin lipid film that was then completely dried overnight in a continuously pumped vacuum. To make the liposome suspension, 4 ml of buffer (10 mM Hepes, 10 mM NaCl, pH 7.2) was added at a temperature 10°C above the phase transition of the lipid mixture, and the sample was maintained at the same temperature for 2 h to achieve complete lipid hydration. The suspension of lipid multilayers was then rapidly frozen in liquid nitrogen and thawed at room temperature three times to allow preformed small liposomes to fuse with the multilayers. This procedure was then followed by extrusion of the dispersion through a multipore filter (100-nm-diameter pores). The extruder and the lipid sample were kept at all times 10°C above the phase transition of the lipid mixture. Each sample was prepared at least in duplicate. Liposomes were annealed for 12 h before use in experiments. At room temperature quasi-elastic light scattering usually showed one well-defined liposome population with an average liposome diameter of 140 ± 30 nm. Lipid content was determined by the method of Bartlett (1959).

Fluorescence measurements

The absorbance of each sample was adjusted to be less than 0.06 to eliminate possible artifacts from light scattering and internal filter effects. All fluorescence spectra were recorded on an SLM/8000C Aminco spectrofluorimeter (Urbana, IL), and lifetimes were determined on an ion-scattered spectroscopy–modified 4800 spatial light modulator. The excitation wavelength was 350 nm; emission spectra were recorded from 360 to 650 nm. Spectra were corrected for instrument response, and integral intensities were used in all cases. For each DMPC–DSPC mixture the cooling temperature scan started 10–15°C above the fluidus and finished at 15°C. The temperature was controlled to an accuracy of ±0.1°C. Temperatures were changed in 2.5°C steps, with an equilibration time at each temperature of 15 min.

RESULTS AND DISCUSSION

Experimental

Quenching data at constant total system composition were obtained as a function of temperature for the various DMPC–DSPC mixtures. Analysis of the data was carried out at constant temperature, however, because at constant temperature the compositions of coexisting gel and fluid phases are constant, with only the fractions of both phases varying. Fig. 1A shows the set of quenching data obtained at 35°C. Qualitatively the same behavior was observed at all the temperatures examined. The conditions of composition and temperature at which the complete data set was obtained are shown in Fig. 1 *B*. Two conclusions can be drawn from the complete data set and are evident in the sample data at 35°C in Fig. 1 *A*:

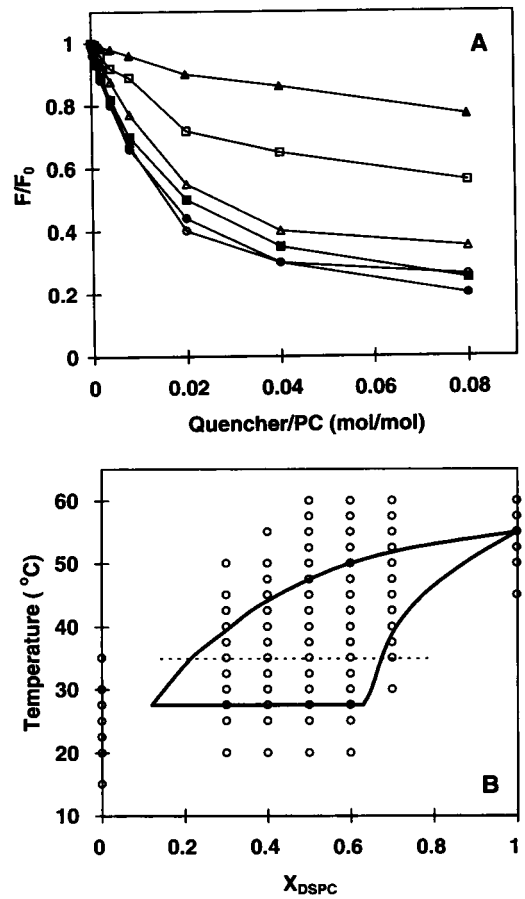

FIGURE 1 (*A*) Fluorescence quenching of DPH-PC by SL-DMPC in large unilamellar vesicles at 35°C at different fractions of the fluid phase, X_{fluid}. The fluorophore/total PC molar ratio was kept constant at 1/500 in all cases. F is fluorescence intensity with quencher; F_0, that without quencher. X_{fluid}: ●, 1; ○, 0.83; △, 0.61; □, 0.38; ▲, 0.17; ■, 0. (*B*) Summary of the experimental data. Each circle in the phase diagram represents the point where the fluorescence spectrum was taken. Data presented in (*A*) lie on the dashed curve.

1) Fluorescence quenching in the all-fluid and all-gel phases is almost the same. This is not particularly surprising, because in both quenching occurs in a single-phase, homogeneous bilayer and depends only on the fluorophore/quencher molar ratio. Measured lifetimes and quantum yields are similar in fluid and gel phases, with the gel phase ~20% higher than the fluid phase (data not shown). It can be calculated from the values of the lateral diffusion coefficient in the fluid lipid phase ($\sim 10^{-8}$ cm^2 s^{-1}; Almeida and Vaz, 1995) that the hopping frequencies between nearest-neighbor sites is of the order 100 ns (Galla and Sackmann, 1974) and that the diffusion in the gel phase is even slower (10^{-10} cm^2 s^{-1}; Cevc and Marsh, 1987). Inasmuch as measured lifetimes in both phases are ~6 ns, which is much less than the time required for a single diffusion jump, observed quenching must be static in both all-fluid and all-gel phases. This is also in the agreement with the conclusion of London and Feigenson (1981), who examined DPH-PC quenching by a spin-labeled lipid in hen

egg phosphatidylcholine bilayers. Observed fluorescence quenching is static not only in terms of the lateral diffusion but also in terms of respective orientations of fluorophore and quencher during the fluorophore lifetime. Rotation correlation times for the acyl chains measured for DPPC in gel and fluid phases are of the order of 1–100 ns (Cevc and Marsh, 1987), so no substantial rotation or change of the depth localization of the quencher, the fluorophore, or both during the lifetime of the fluorophore occurs. The efficiency of the fluorescence quenching in the SL-DMPC–DPH-PC pair seems to be position and orientation dependent. This dependency probably explains the relatively high values of the residual fluorescence observed in the single-phase, homogeneous systems. There is some experimental evidence to support this. When ^{6}SL-DMPC is used as quencher in the equimolar DMPC/DSPC mixture, the plateau value of F/F_0, the residual fluorescence, of DPH-PC in the all-fluid phase is substantially higher than when ^{13}SL-DMPC is used. In addition, when the liposomes are formed exclusively from the ^{13}SL-DMPC, the residual fluorescence value is still at 0.07 (data of both experiments not shown).

2) In the region of two-phase coexistence, the main contribution to the observed phenomenon comes from the fluid phase. As can be clearly seen from the sample data plotted for 35°C in Fig. 1 *A* and from similar data obtained for other temperatures, fluorescence quenching in this region is less than in the homogeneous, single-phase systems, and a residual fluorescence persists that is significantly higher than the residual fluorescence in the single-phase, homogeneous systems. This result can be explained either on the basis of changes of the relative concentrations of fluorophore and quencher in the fluid phase or by a drastic change in the fluorescence-quenching process itself. We can reject the latter explanation because the fluorescence lifetimes and quantum yields in fluid and gel phases are similar, with the quantum yield in the gel phase only ~20% higher than that in the fluid phase. This situation cannot be changed simply by the division of the membrane plane into gel- and fluid-phase compartments. The mean concentrations of fluorophore and quencher in the fluid phase at constant temperature are constant for the following reasons: The distribution constant for DPH-PC between these two phases, $K_{f/g} = 3.3$, does not depend either on the overall DMPC–DSPC composition or on the temperature (Parente and Lentz, 1985). In addition, at the constant temperature the compositions of the coexisting phases, given by the phase diagram, are constant. Thus the only variable that changes in the sample data set plotted in Fig. 1 *A* and in any other constant-temperature plot is the fluid-phase fraction, X_{fluid}. In contrast to that for the mean fluorophore and quencher concentrations in the fluid phase, disconnection of this phase into isolated fluid domains strongly affects their relative local concentrations in the closed domains and thus the observed total fluorescence quenching as documented in Fig. 1 *A*. It can be understood qualitatively based on the following considerations. Earlier work in the DMPC–DSPC system has shown that the locus of percolation thresholds lies near the liquidus, and thus the fluid phase is disconnected over most of the two-phase region (Vaz et al, 1989). It is also known that the average domain size in this system is only hundreds of molecules (Sankaram et al., 1992). Many domains will therefore contain no fluorophore, although they may contain a few or many quenchers, especially at high quencher concentrations. Therefore, because the disconnected fluid domains are closed and unconnected to one another, the effective quencher concentration in the fluid domains as a group is much reduced. For a given temperature, there exists a fluid-phase fraction, X_{fluid}^{percol}, at which quenching begins to differ significantly from that at the all-fluid phase. These fluid fractions–percolation thresholds, X_{fluid}^{percol}, obtained from the data of Fig. 1 *A* and from similar data for other temperatures, are plotted as filled circles in the phase diagram shown in Fig. 2. The loci of these points are in good agreement with the percolation threshold locus (dashed curve) determined by fluorescence recovery after photobleaching (FRAP) (Vaz et al, 1989) and electron paramagnetic resonance (Sankaram et al., 1992). It should also be pointed out that percolation behavior may occur under some conditions when the disconnected fluid-phase domains are large enough to contain enough fluorophore molecules that each domain mimics the behavior of the whole system. From the experimental point of view, a one-phase system with a continuous fluid phase and a system with the fluid phase disconnected into large domains are indistinguishable. This condition is most likely to occur just after disconnection of the fluid phase because the results of the simulations, discussed below, show that the average domain size decreases with decreasing fraction of the fluid phase.

Fluorescence in the discontinuous gel phase is much less, mainly as a result of to the lower fluorophore and quencher occupancy of this phase; thus the gel-phase domains contribute only a quasi-constant, low background to the observed fluorescence. This is documented also in Fig. 1 *A*, where curve of F/F_0 obtained with the fluid-phase fraction

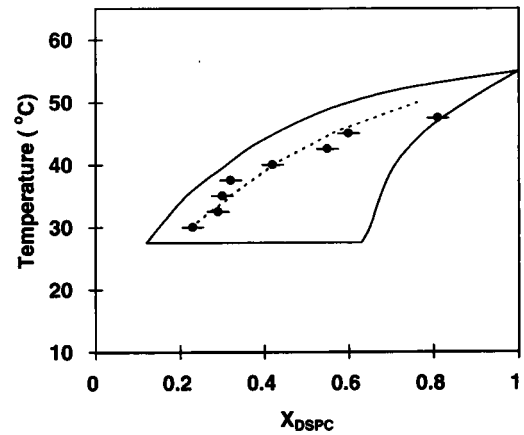

FIGURE 2 Percolation threshold values (●) obtained from the fluorescence-quenching data. The dashed curve is the percolation threshold locus from the FRAP experiments of Vaz et al. (1989).

$X_{fluid} = 0.83$ shows only insignificant deviations from the fluorescence quenching observed in the single fluid phase.

The preceding discussion focused on the behavior of a single bilayer in a large unilamellar vesicle. The actual system under observation, however, consists of an aqueous dispersion of a very large number of vesicles, each one of which is, by itself, a small system. The vesicle dispersion thus constitutes a large dispersed lipid phase in a continuous aqueous phase. With this viewpoint in mind, consider a dispersion with the fluid phase continuous as it nears the percolation threshold at constant temperature, by variation of the composition. As noted above, under these conditions the relative amounts of the two phases change, but their compositions do not. Inasmuch as each vesicle bilayer is a small, finite system, all vesicles will not reach their percolation thresholds at exactly the same total system composition. Thus the percolation threshold of the dispersion will be distributed along the composition axis. This distributed character can actually be directly observed in FRAP experiments on supported multibilayers in which the stack of bilayers is the analog of the vesicle dispersion (Almeida et al., 1993). From an operational standpoint, in the fluorescence-quenching experiments the vesicle dispersion will be said to percolate when the values of F/F_0 in the two-phase region differ detectably from the values of this parameter in the continuous-fluid system. At constant temperature, the distributed nature of the percolation threshold along the composition axis together with the decrease in disconnected fluid domain size with decreasing fluid fraction may cause the operationally distributed percolation threshold to shift to lower fluid fractions. The shift of the percolation thresholds values to the lower fluid phase fractions is evident in Fig. 2 in the data derived from the fluorescence-quenching experiments at higher temperatures.

Simulations

To understand the experimental data better, we performed a series of simple simulations, using a model similar to that used in simulations of FRAP experiments (Schram et al., 1994). The lipid bilayer was simulated on a triangular lattice with 100 x 100 sites with a periodic boundary condition in which fluorophore and quencher were distributed randomly and independently. On this triangular lattice each site located the position of a single acyl chain, not a molecule. Diffusion was simulated by the random exchange of neighboring chains. Quenching occurred when a quencher site was detected in the two nearest layers around the fluorophore site. Note that efficiencies of quenching = 1 and quantum yield = 1 are introduced in this way, which is not necessarily true for the experimental system. We determined the intensity of fluorescence simply by counting the unquenched fluorophores. The compartmentalized system in our simulations consisted of a compartmentalized and a continuous part, which were simulated independently (on the different lattices); then we assembled the whole system as a linear combination of both parts, using Eq. 1 below. The continuous part of the system was simulated as described above. In a given simulation for the compartmentalized part of the system the entire lattice was divided into compartments, which were all closed, and each compartment was of the same size corresponding to $m \times m$ sites (where $m = 3, 5, 8, 18, 31$). The random distribution of quenchers and fluorophores over the whole lattice created the nonhomogeneous occupancy of the compartments by both types of molecule. Fluid and gel phases were simulated by use of numbers of quencher- and fluorophore-labeled sites corresponding to the actual distribution of fluorophore and quencher between two coexisting phases in the experimental systems. For each experimental condition (see Fig. 1 *B*) we generated the corresponding simulated quenching curve from the continuous and discontinuous lattices, assuming that

$$(F_{total}/F_0) = (X_{fluid}F_{fluid} + X_{gel}F_{gel})/F_0. \quad (1)$$

The fractions of fluid and gel phases, X_{fluid} and X_{gel}, were obtained from the phase diagram; fluorescence intensities for the fluid and gel phases, F_{fluid} and F_{gel}, from the simulations. F_0 is the total number of fluorophore molecules used. In this way the only free variable is the size of the compartments, n ($n = m \times m$ sites), in the discontinuous phase. The percolation threshold locus obtained in the FRAP experiments by Vaz et al. (1989) (dashed curve in Fig. 2) was used as a criterion for continuity of the gel or fluid phases: if $X_{fluid} > X_{percol}$ at a given temperature, the fluid phase was considered continuous; if $X_{fluid} < X_{percol}$ at a given temperature, the continuous phase was a gel.

As a simple test of the viability of the model, the simulated and experimental curves for the homogeneous phase were compared. First, however, all experimental curves were corrected for the residual fluorescence of the fluid phase at high quencher concentrations which is probably due to the lower efficiency of the quenching than was considered to be the case in the simulations. The correction was done as follows: The value of the fluorescence intensity for the all-fluid system at the plateau ($F/F_0 = 0.2$) was subtracted from each curve, and the curve was then renormalized from 0 to 1:

$$(F/F_0)_{corrected} = ((F/F_0)_{experimental} - 0.2)/0.8. \quad (2)$$

As illustrated by Fig. 3A, both experimental (●) and simulated (○) curves are in good agreement.

To examine the effect of compartmentalization we generated a set of simulated curves for different compartment sizes, n, for a given phase state of the system, using the procedure described above. This set was then compared with the experimental data for the same system corrected for the residual fluorescence of the fluid phase by use of Eq. 2. The simulated curve best fitting the experimental data within the experimental error was then selected as the representative one, and the corresponding size of the domain, n, was noted. If such a simulated curve was not

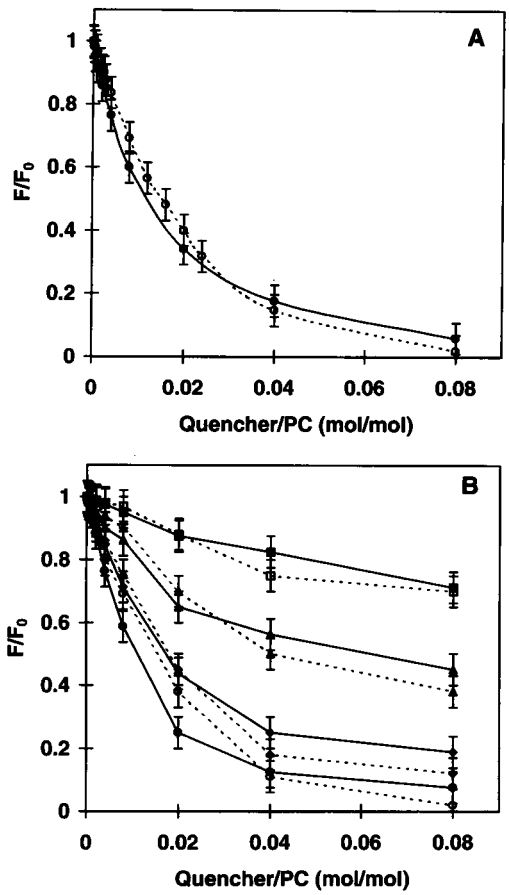

FIGURE 3 (*A*) Comparison of the simulated fluorescence-quenching curve (○) with the experimental quenching curve (●). The experimental curve was corrected for the residual fluorescence of the fluid phase at high quencher concentration, as explained in the text. (*B*) Comparison of the simulated and experimental quenching curves at 35°C. The simulated curves (*dashed curves*) were generated from the separate simulations of the gel and fluid phases by use of Eq. 1, as explained in the text, and the experimental curves (*solid curves*) were corrected for the residual fluorescence of the fluid phase at high quencher concentration. Fluid phase fraction, X_{fluid}, for the experimental curves: ●, 0.83; ♦, 0.61; ▲, 0.38; ■, 0.17. The corresponding fluid domain sizes expressed in the number of sites, $n^{(1)}_{fluid}$, for given X_{fluid} are ○, continuous fluid; ◇, 961; △, 324; □, 9.

available because of the limited number of compartment sizes simulated, the estimation was not made. An example of the simulated set of data for the compartmentalized system is shown in Fig. 3 *B*, in which both of the experimental curves obtained at 35°C, corrected for the residual fluorescence plateau (Eq. 2), and corresponding representative simulated curves are shown. The estimated sizes of the fluid-phase compartments, n_{fluid}, found in the complete set of experimental data are summarized in Table 1 as a function of the fluid fraction in the system, X_{fluid}, at different temperatures. As can be clearly seen from this table, the sizes of the compartments increase with an increase in the fraction of the fluid phase in the system at any given temperature, which is in qualitative agreement with observations of Sankaram et al. (1992).

TABLE 1 Size of the fluid phase domains, n_{fluid}, as a function of the fluid phase fraction, X_{fluid}, for different temperatures

Temperature (°C)	X_{fluid}	$n^{(1)}_{fluid}$*	$n^{(2)}_{fluid}$#
30	0.29	9	5
	0.5	25	13
	0.71	64	32
32.5	0.14	9	5
	0.35	9	5
	0.55	25	13
35	0.17	9	5
	0.38	324	162
	0.61	961	481
37.5	0.22	9	5
	0.44	961	481
40	0.07	9	5
	0.3	25	13
42.5	0.12	324	162

*The sizes of fluid phase domains, expressed as the number of the lattice sites, $n^{(1)}_{fluid}$, were determined by direct comparison of the simulated and experimental curves, as explained in the text.
#The sizes of fluid phase domains expressed as the number of lipid molecules, $n^{(2)}_{fluid}$, were obtained as $n^{(1)}_{fluid}/2$.

In summary, it is clear that the decrease in the fluorescence quenching in the two-phase coexistence region of a DMPC–DSPC mixture compared with that in the single-phase region must be due to the disconnection of the fluid phase into many isolated domains. This consideration is strengthened by the simulation results. The location of the percolation threshold locus on the phase diagram for the system deduced from the fluorescence-quenching data agrees well with the location determined by FRAP (Vaz et al., 1989) and electron spin resonance (Sankaram et al., 1992). In addition, the combination of experimental and simulation data leads to the conclusion that fluid domain size increases with increasing fluid fraction at constant temperature. This conclusion is in accord with that reached by Sankaram et al. (1992), although in their electron spin resonance experiments the fluid fraction was varied by change of temperature at fixed total system composition.

We thank Dr. Vincent Schram for his help with the simulations. This research was supported by National Institute of Health grants GM-14628 and GM-25373.

REFERENCES

Almeida, P. F. F., and W. L. C. Vaz. 1995. Lateral diffusion in membranes. *In* Handbook of Biological Physics, Vol. 1. R. Lipowsky and E. Sackmann, editors. Elsevier Science B. V., Amsterdam. 305–357.

Almeida, P. F. F., W. L. C. Vaz, and T. E. Thompson. 1993. Percolation and diffusion in three-component lipid bilayers: effect of cholesterol on an equimolar mixtures of two phosphatidylcholines. *Biophys. J.* 64: 399–412.

Bartlett, G. R. J. 1959. Phosphorous assay in column chromatography. *J. Biol. Chem.* 234:466–468.

Cevc, G., and D. Marsh. 1987. Bilayer phase transitions. *In* Phospholipid Bilayers. Physical Principles and Models. John Wiley & Sons, New York. 235, 375.

de Bony, J., A. Lopez, M. Gilleron, M. Welby, G. Laneelle, B. Rousseau, J.-P. Beaucourt, and J.-F. Tocanne. 1989. Transverse and lateral distribution of phospholipids and glycolipids in the membrane of the bacterium *Micrococcus luteus*. *Biochemistry*. 28:3728–3737.

Edidin, M. 1992. The variety of cell surface membrane domains. *Comments Mol. Cell. Biophys.* 8:73–82.

Edidin, M., and I. Stroynowski. 1991. Differences between the lateral organization of conventional and innositol phospholipid-anchored membrane proteins. A further definition of micrometer scale domains. *J. Cell Biol.* 112:1143–1150.

Galla, H.-J., and E. Sackmann. 1974. Lateral diffusion in the hydrophobic region of membranes: use of pyrene excimers as optical probes. *Biochim. Biophys. Acta.* 339:103–115.

Lakowicz, J. R. 1983. Quenching of fluorescence. *In* Principles of Fluorescence Spectroscopy. Plenum Press, New York. 258–304.

London, E., and G. W. Feigenson. 1981. Fluorescence quenching in model membranes. 1. Characterization of quenching caused by a spin-labeled phospholipid. *Biochemistry*. 20:1932–1938.

Marsh, D., and A. Watts. 1982. Spin labeling and lipid-protein interactions in membranes. *In* Lipid-Protein Interactions, Vol. 2. P. Jost and O. H. Griffith, editors. John Wiley & Sons, New York, 53–126.

Melo, E. C. C., I. M. G. Lourtie, M. B. Sankaram, T. E. Thompson, and W. L. C. Vaz. 1992. Effects of domain connection and disconnection on the yields of in-plane bimolecular reaction in membranes. *Biophys. J.* 63: 1506 -1512.

Pagano R. E., and R. G. Sleight. 1985. Defining lipid transport pathways in animal cells. *Science*. 229:1051–1057.

Parente, R. A., and B. R. Lentz. 1985. Advantages and limitations of 1-palmitoyl-2-[[2-[4-(6-phenyl-*trans*-1,3,5-hexatrienyl)phenyl]ethyl-]carbonyl]-3-*sn*-phosphatidylcholine as a fluorescent membrane probe. *Biochemistry*. 24:6178–6185.

Sankaram, M. B., D. Marsh, and T. E. Thompson. 1992. Determination of fluid and gel domain sizes in two-component, two-phase lipid bilayers. An electron spin resonance spin label study. *Biophys. J.* 63:340–349.

Schram, V., J.-F. Tocanne, and A. Lopez. 1994. Influence of obstacles on lipid lateral diffusion-computer simulation of FRAP experiments and application to proteoliposomes and biomembranes. *Eur. Biophys. J.* 23:337–348.

Singer, S. J., and G. L. Nicolson. 1972. The fluid mosaic model of the structure of cell membranes. *Science*. 175:720–731.

Thompson, T. E., M. B. Sankaram, and R. L. Biltonen. 1992. Biological membrane domains: functional significance. *Comments Mol. Cell. Biophys.* 8:1–15.

Thompson, T. E., M. B. Sankaram, R. L. Biltonen, D. Marsh, and W. L. C. Vaz. 1995. Effects of domain structure on in-plane reactions and interactions. *Mol. Membr. Biol.* 12:157–162.

Tocanne, J.-F. 1992. Detection of lipid domains in biological membranes. *Comments Mol. Cell. Biophys.* 8:53–72.

Tocanne, J.- F., L. Dupou-Cezanne, A. Lopez, and J.- F. Tournier. 1989. Lipid lateral diffusion and membrane organization. *FEBS Lett.* 257: 10–16.

Vaz, W. L. C. 1994. Diffusion and chemical reactions in phase-separated membranes. *Biophys. Chem.* 50:139–145.

Vaz, W. L. C., E. C. C. Melo, and T. E. Thompson. 1989. Translational diffusion and fluid domain connectivity in a two-component, two-phase phospholipid bilayer. *Biophys. J.* 56:869–876.

Welti, R., and M. Glaser. 1994. Lipid domains in model and biological membranes. *Chem. Phys. Lipids.* 73:121 -137.